



Dynamic model for simulating transient behaviour of rotary drum granulation loop

L. Vesjolaja¹ B. Glemmestad² B. Lie¹

¹Department of Electrical Engineering, IT and Cybernetics, University of South-Eastern Norway.
E-mail: {ludmila.vesjolaja, bernt.lie}@usn.no

²Process Modeling and Control Department, Yara Technology Center, Norway. E-mail:bjorn.glemmestad@yara.com

Abstract

In this paper, a dynamic model for a rotary drum granulation loop with external product separator is developed. A population balance is used to capture dynamic particle size distribution in the 3-compartment rotary drum granulator model. Particle agglomeration along with particle growth due to layering are assumed as granulation mechanisms in the rotary drum. The model of the granulation loop includes models of the drum, screens and a crusher. Simulations using the developed model provide valuable data on dynamic fluctuations in the inlet and the outlet particle size distribution for the rotary drum. Simulation results showed that at smaller crusher gap spacings, the instabilities of the drum granulation loop occur, and damped oscillations are observed. Above the critical crusher gap spacing, sustained periodic oscillations are observed. The reason for oscillations is the off-spec particle flow that is recycled back to the granulator.

Keywords: granulation loop; population balance; layering; agglomeration

1 Introduction

Granulation processes are used in a wide range of industrial applications, such as those in pharmaceutical and fertilizer industries (Litster and Ennis, 2004). This paper is focused on the last part of NPK (Nitrogen, Phosphorus, Potassium) fertilizer production. A granulation loop is used to produce different grades, i.e., various N:P:K ratios, of fertilizers. The NPK fertilizer is a high value type of fertilizer containing the three main elements essential for crop nutrition. Various NPK grades are specially developed for different crops growing in different climates and soils. Fertilizer manufacturing using the granulation process has received considerable research interest during the last few decades, due to (i) the increasing requirements for efficient production of high quality fertilizers for increased food production in a growing global population, (ii) difficult process control and operation, e.g.,

among others Bück et al. (2016); Ramachandran and Chaudhury (2012); Herce et al. (2017); Ramachandran et al. (2009); Valiulis and Simutis (2009); Wang et al. (2006) and Cameron et al. (2005) have focused their research on granulation processes. The granulation loop studied in this paper consists of a rotary drum granulator, a granule classifier (screens), and a roll crusher. A typical schematic of a granulation process with a recycle loop is shown in Figure 1. Rotary drums as granulation units are frequently used in fertilizer industries due to the ability of rotary drums to handle large amount of material.

During the granulation process, a slurry of liquid ammonium nitrate and partly dissolved minerals is solidified to form granules. Granules that are too small (under-sized particles) are recycled to the granulation unit and granules that are too large (over-sized particles) are first crushed and then recycled back to the granulator. The recycle feed is an integral part of the

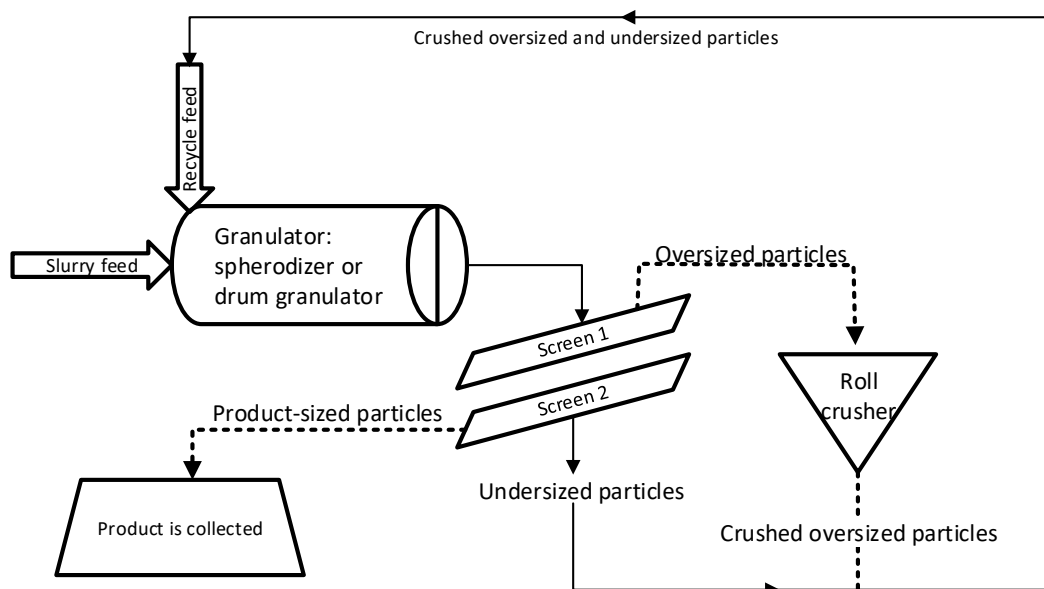


Figure 1: Schematic diagram of granulation loop.

granulation process. The recycle feed flow rate as well as its particle size distribution (PSD) are important for proper process operation. The recycle of off-spec (under-sized and over-sized) particles is needed to seed the granulator. Another reason to recycle the feed is a wide PSD of the granules at the granulator discharge. Typically, the PSD of the granules leaving the granulator is wider compared to the required PSD of the final product. In addition, the off-spec granules cannot be considered as a waste material, and must be recycled from an economic and environmental point of view. Unfortunately, for some granulation technologies, the amount of the recycled material is large. A typical recycle ratio in granulation plants is 4:1. This implies a high ratio between the off-spec particles ($\sim 80\%$) and the required product size particles ($\sim 20\%$).

Process control of granulation loops is challenging. Granulation loops may show oscillatory behavior for certain operating points. Instability is linked to the entire granulation loop, since the granulator receives as input a fluctuating recycled stream. Similar oscillations in granulation loop are reported in Drechsler et al. (2005) and Radichkov et al. (2006); the authors have analyzed granulation loop dynamics for fluidized bed granulators. Particle size change in fluidized beds has been assumed to be caused by particle layering and attrition mechanisms. Particle agglomeration is neglected in Drechsler et al. (2005) and Radichkov et al. (2006).

The contributions of this paper are (i) proposing a control relevant model of the granulation loop with a rotary drum granulator, (ii) including both particle agglomeration and particle growth by layering in the rotary drum model by using a population balance equation, (iii) developing a 3-compartment rotary drum model for simulations of granulation loop, and (iv) analyzing and suggesting possible improvements for stability of the drum granulation loop.

The paper is organized as follows: In Section 2, a mathematical model of a granulation loop, including models of a rotary drum, screens, and a crusher, is given. In Section 3, the numerical solution methods for the developed model are provided. Simulation setup, results, and discussions are given in Section 4, while conclusions are drawn in Section 5.

2 Model development

2.1 Model for granulator

In this study, population balance principles have been used to develop a mathematical model of a granulator suitable for control purposes. Population balance (PB) is frequently used to describe dynamics of particle property distributions. In the granulator model, a mass based population balance equation (PBE) with particle diameter as the internal coordinate is used. This choice of PBE is made because the PSD in a real

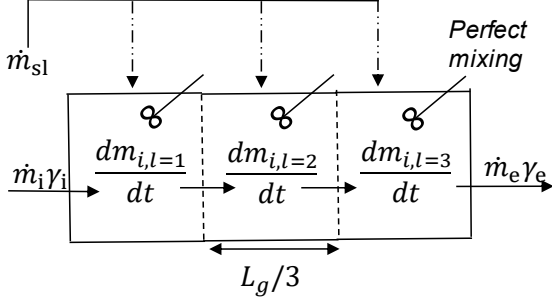


Figure 2: Multi-compartment rotary drum model.

plant is typically measured by sieving and weighting. The general form of a mass based PBE with particle diameter (L) as the internal coordinate, spatial variation (z) as the external coordinate, and time coordinate (t) is represented as

$$\frac{\partial m(L, z, t)}{\partial t} = -L^3 \frac{\partial}{\partial L} \left[G \frac{m(L, z, t)}{L^3} \right] + B(L, z, t) - D(L, z, t) - \frac{\partial}{\partial z} \left[\frac{dz}{dt} m(L, z, t) \right], \quad (1)$$

where $m(L, z, t)$ is the mass density function, L is the particle diameter, G is the particle growth rate, B is the particle birth rate, and D is the particle death rate (Ramkrishna, 2000). The first term on the right hand side represents the particle growth due to layering, the second and third terms stand for particle birth and death, respectively, due to agglomeration, and the last term represents a continuous process and gives the flow of particles through the granulator. Equation 1 is derived by assuming that all particles are ideal spheres with a constant solid density.

Particle growth due to layering (G) is a continuous process during which particle growth occurs by successive coating of a liquid phase onto a granule (Litster and Ennis, 2004; Iveson et al., 2001). In a given case, a fresh fertilizer melt (slurry) is added to the rotary drum to ensure particle growth. As a result, the particle mass grows, and the volume increases, but the number of particles in the system remains unchanged. Assuming a size-independent linear growth (Mörl, 1981; Mörl et al., 1977), i.e., assuming that each granule has the same exposure to a slurry material, the layering term is modeled as

$$G = \frac{2\dot{m}_{sl}(1 - X_{sl,i})}{\rho A_{p,tot}}, \quad (2)$$

$$A_{p,tot} = \pi m \int_{L=0}^{L=\infty} L^2 dL. \quad (3)$$

Here, m is the mass of the particles, \dot{m}_{sl} is the slurry flow rate, $X_{sl,i}$ is the moisture fraction in the slurry, and $A_{p,tot}$ is the total surface area of the particles as given by Equation 3.

In rotary drum granulators, particle collision cannot be avoided, and thus should be included in the model. In this paper, for simplicity, binary particle agglomeration is assumed. Binary agglomeration refers to a granulation mechanism that occurs due to successful collision of two particles, resulting in the formation of a larger, composite particle. Agglomeration is a discrete (sudden) process event that changes the total number of particles: two particles *die*, and a new particle is *born* as a result of collision of two particles. Thus, the agglomeration results in a reduction of the total number of particles, while the total mass remains conserved (Litster and Ennis, 2004; Iveson et al., 2001). Here, the particle birth (B) and death (D) due to binary agglomeration are modeled using Hulburt and Katz' formulation (Hulburt and Katz, 1964). The B and D terms in Equation 1 are modeled using Equation 4 and 5, respectively.

$$B = \frac{L^2}{2} \int_0^L \frac{\beta \left((L^3 - \lambda^3)^{\frac{1}{3}}, \lambda, t \right) \cdot m \left((L^3 - \lambda^3)^{\frac{1}{3}}, t \right) \cdot m(\lambda, t)}{(L^3 - \lambda^3)^{\frac{2}{3}}} d\lambda, \quad (4)$$

$$D = m(L, t) \int_0^\infty \beta(L, \lambda) m(\lambda, t) d\lambda. \quad (5)$$

Here, the B term represents the particle birth of diameter L , while the D term represents the disappearance (death) of particle of diameter L , and β is the agglomeration rate (kernel) that defines the collision frequency of the two particles with diameters λ and $L - \lambda$. In this paper, the agglomeration kernel is defined using the Kapur agglomeration kernel model (Kapur, 1972) by taking $a = 2$ and $b = 1$:

$$\beta = \left(\frac{6}{\pi} \right)^{\frac{2}{3}} \frac{1}{\rho} \beta_0 \beta_{jk}, \quad (6)$$

where the term $\left(\frac{6}{\pi} \right)^{\frac{2}{3}} \frac{1}{\rho}$ arises during the conversion from a number-based formulation to the mass-based formulation of PBEs, β_0 is the particle size independent part of the agglomeration kernel, and β_{jk} is the particle size dependent part of the agglomeration kernel as shown in Equation 7.

$$\beta_{jk} = \frac{(L_j + L_k)^2}{L_j L_k}. \quad (7)$$

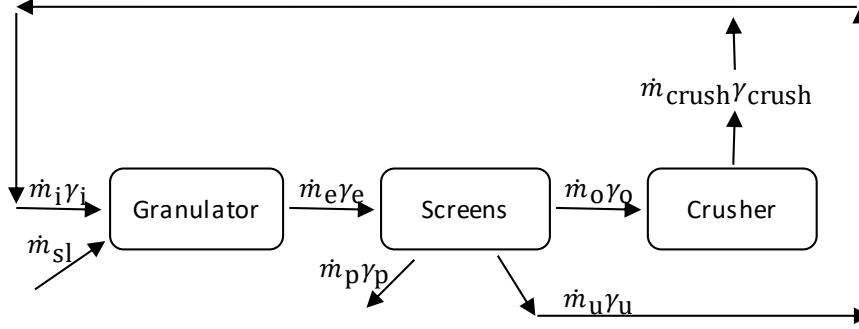


Figure 3: Simplified flow diagram of the drum granulation loop. Here, \dot{m}_{sl} is the slurry flow rate, \dot{m}_i , \dot{m}_e , \dot{m}_o , \dot{m}_u , \dot{m}_p , \dot{m}_{crush} are the mass flow rates of influent, effluent, over-sized, under-sized, product-sized and crushed particles respectively. The corresponding distribution functions of the influent, effluent, over-sized, under-sized, product-sized and crushed particles are denoted with γ_i , γ_e , γ_o , γ_u , and γ_p , γ_{crush} , respectively.

The effluent from the granulator is calculated by assuming a 3-compartment granulator model. For this, the length of the granulator L_g is divided into 3 equally sized sections (compartments) which are numbered by $l \in \{1, 2, 3\}$, as shown in Figure 2. In each of the compartments the concept of *perfect mixing* is assumed. The influent to the granulator (recycled particles), \dot{m}_i , enters the 1st compartment and the effluent, \dot{m}_e , leaves the granulator from the 3rd (last) compartment. The particle velocity is assumed constant in all three compartments and is calculated as

$$\frac{dz}{dt} = \frac{L_g}{\tau}, \quad (8)$$

where τ is the particle retention (residence) time in the granulator.

2.2 Model for upper and lower screen

The mass flow rates out from the screens are described using probability function P_{upp} and P_{low} from Molerus and Hoffmann (1969). If P is the probability with which particles remain lying on the screen (do not pass the screen) and $(1 - P)$ is the probability with which particles pass through the screen, then the mass flow rates from the screen are calculated as

$$\dot{m}_o \gamma_o = P_{upp} \dot{m}_e \gamma_e, \quad (9)$$

$$\dot{m}_u \gamma_u = (1 - P_{upp}) (1 - P_{low}) \dot{m}_e \gamma_e, \quad (10)$$

$$\dot{m}_p \gamma_p = (1 - P_{upp}) P_{low} \dot{m}_e \gamma_e. \quad (11)$$

Here, \dot{m}_o , \dot{m}_u , \dot{m}_p are the mass flow rates of over-sized, under-sized, and product-sized particles, respectively. The corresponding distribution functions of the over-sized, under-sized, and product-sized particles are denoted with γ_o , γ_u , and γ_p , respectively. The screening probability functions P_{upp} and P_{low} defined by Molerus and Hoffmann (1969) and also given in Heinrich et al. (2003) are calculated using Equation 12 and 13.

$$P_{upp} = \frac{1}{1 + \left(\frac{L_{m,upp}}{L}\right)^2 \exp\left(K_{eff,upp} \left(1 - \left(\frac{L}{L_{m,upp}}\right)^2\right)\right)}, \quad (12)$$

and

$$P_{low} = \frac{1}{1 + \left(\frac{L_{m,low}}{L}\right)^2 \exp\left(K_{eff,low} \left(1 - \left(\frac{L}{L_{m,low}}\right)^2\right)\right)}, \quad (13)$$

where L_m is the mesh size of the screen (sieve diameter), L is the particle diameter, and K_{eff} is the screen separation efficiency.

2.3 Model for crusher

A mathematical model of the crusher represents the distribution function (Equation 14) that re-distributes the total over-sized mass flow ($\dot{m}_o \gamma_o$) with the new distribution function γ_{crush} . This distribution function γ_{crush} reassigns the net over-sized flow rate to lower sized classes. Having a crusher gap spacing and a standard deviation as design choices, the crusher distribu-

tion function is defined as

$$\gamma_{\text{crush}} = \frac{1}{\sqrt{2\pi\sigma_{\text{crush}}^2}} \exp\left(-\frac{(L - L_{\text{crush}})^2}{2\sigma_{\text{crush}}^2}\right). \quad (14)$$

Here, σ_{crush} is the standard deviation, and L_{crush} is the crusher diameter, which is the mean size of the crushed particle distribution such that $L_{\text{crush}} > 0$. In addition, L is bounded, $0 < L \leq L_{\text{max}}$. For proper choice of σ_{crush} , L_{crush} and L , $\gamma_{\text{crush}} \geq 0$. The total over-sized particle flow rate is then calculated as

$$\dot{m}_{\text{crush}} \gamma_{\text{crush}} = \left(\sum \dot{m}_o \gamma_o\right) \cdot \gamma_{\text{crush}}. \quad (15)$$

The mass flow rate that is recycled back to the granulator, i.e., the mass flow of the off-spec particles, is given as

$$\dot{m}_i \gamma_i = \dot{m}_{\text{crush}} \gamma_{\text{crush}} + \dot{m}_u \gamma_u. \quad (16)$$

The overall balance scheme for the drum granulation loop is given in Figure 3.

3 Model solution

The solution to PBEs is found by transforming the partial differential equation (PDE) into a system of ordinary differential equations (ODEs) that further can be solved using an appropriate time integrator. The PDEs for PBE are discretized in terms of the internal coordinate, i.e., particle diameter, and also in terms of the external coordinate, i.e., the length of the drum granulator. The discretization is 2-dimensional. For the internal coordinate discretization, particles are classified into N_i particle classes using a linear grid and are numbered by $i \in \{1, 2, \dots, N_i\}$. On the other hand, for the external coordinate discretization, the granulator length in axial direction is divided into l equally sized compartments (sections) and are numbered by $l \in \{1, 2, 3\}$.

Numerical solution for the layering term $L^3 \frac{\partial}{\partial L} \left[G \frac{m(L,z,t)}{L^3} \right]$ is found by applying a high resolution finite volume scheme. In particular, a finite volume scheme extended by a Koren flux limiter function is used to discretize the layering term in terms of its internal coordinate. The Koren flux limiter scheme is described in Koren (1993) and applied for granulation process in Vesjolaja et al. (2018).

Finding a sufficiently accurate solution for the agglomeration terms (Equation 4 and 5) is challenging. Agglomeration is a discrete event, and as shown by Equation 4 and 5, PB modeling of the agglomeration terms result in partial integro-differential equations. In this paper, approximation of the birth and death terms is performed by applying one of the sectional schemes. In particular, the cell average scheme that is introduced

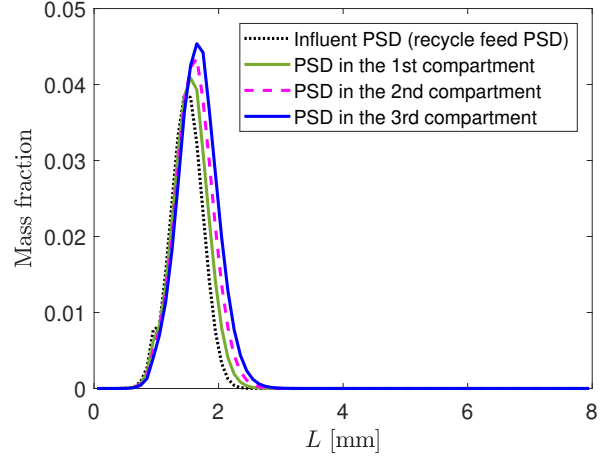


Figure 4: PSD in the 1st, 2nd and 3rd compartments of the 3-compartment granulator for $L_{\text{crush}} = 1.5$ mm.

by Kumar et al. (2006) is used to find a numerical solution. A detailed explanation of the cell average scheme is given in Kumar (2006). The cell average scheme has shown higher accuracy and faster solution compared to other frequently used sectional methods as the Hounslow scheme (Hounslow et al., 1988) and the Fixed Pivot scheme (Kumar and Ramkrishna, 1996).

In this paper, the proposed by Kumar et al. (2006) cell average scheme is re-formulated to give a numerical solution for a mass based PBE with the particle diameter as internal coordinate. To achieve this, the zeroth moment (total number of particles), and the third moment (total mass of particles) has been chosen to be conserved (compared to zeroth and first moments for volume based description, Kumar et al. (2006); Kumar (2006)). Mathematical expressions are reported in Vesjolaja et al. (2018).

Spatial discretization of the granulator length is performed by using a high resolution scheme with Koren flux limiter function (KFL). For this, the granulator is divided into N_z uniformly spaced compartments, and each compartment is assumed to be *perfectly mixed*. Integration of the particle flux term for N_z compartments gives

$$\frac{\partial}{\partial z} \left(\frac{dz}{dt} m_{i,z} \right) = w \frac{\partial}{\partial z} (m_{i,z}) = w \left[m_{i,z-\frac{1}{2}} - m_{i,z+\frac{1}{2}} \right], \quad (17)$$

where $\frac{dz}{dt} = w$ is the particle velocity along the granulator and is assumed to be constant inside the granulator. The approximation of the terms $m_{i,z \pm \frac{1}{2}}$ is then performed using a KFL scheme (Koren, 1993). The approximation of the terms $m_{i,z \pm \frac{1}{2}}$ using the KFL scheme

is given by Equation 18 and Equation 19.

$$m_{i,z-\frac{1}{2}} \approx \frac{1}{\Delta z} \left\{ \frac{M_{i,z-1}}{L_i} + \frac{1}{2} \phi \left(\theta_{i-\frac{1}{2}} \right) \right. \\ \left. \times \left(\frac{M_{i,z-1}}{L_i^3} - \frac{M_{i,z-2}}{L_i^3} \right) \right\}, \quad (18)$$

$$m_{i,z+\frac{1}{2}} \approx \frac{1}{\Delta z} \left\{ \frac{M_{i,z}}{L_i} + \frac{1}{2} \phi \left(\theta_{i-\frac{1}{2}} \right) \right. \\ \left. \times \left(\frac{M_{i,z}}{L_i^3} - \frac{M_{i,z-1}}{L_i^3} \right) \right\}, \quad (19)$$

where, M_i is the total mass of the particle in the i^{th} class and $\Delta z = \frac{L_g}{N_z}$ is the length of the each section in the granulator (Figure 2). The limiter function ϕ in Equation 18 and Equation 19 is defined as

$$\phi(\theta) = \max \left[0, \min \left(2\theta, \min \left(\frac{1}{3} + \frac{2\theta}{3}, 2 \right) \right) \right], \quad (20)$$

and parameter θ is defined as

$$\theta_{i-\frac{1}{2}} = \frac{\frac{M_{i,z}}{L_i^3} - \frac{M_{i,z-1}}{L_i^3} + \varepsilon}{\frac{M_{i,z-1}}{L_i^3} - \frac{M_{i,z-2}}{L_i^3} + \varepsilon}, \quad \theta_{i+\frac{1}{2}} = \frac{\frac{M_{i,z+1}}{L_i^3} - \frac{M_{i,z}}{L_i^3} + \varepsilon}{\frac{M_{i,z}}{L_i^3} - \frac{M_{i,z-1}}{L_i^3} + \varepsilon}. \quad (21)$$

The constant ε is a very small number to avoid division by zero, e.g. $\varepsilon = 10^{-8}$.

4 Simulation Results and Discussion

4.1 Simulation Setup

The numerical solution of PBE described by Equation 1 is found by applying the Koren flux limiter scheme and the cell average schemes as discussed in Section 3. Particles are classified into 80 size classes and the drum length is divided into 3 equally sized compartments. Thus, the PDE represented by Equation 1 is transformed into a set of 240 ODEs which are further solved using a 4-th order Runge-Kutta method with fixed time step. Dynamic simulations are performed using MATLAB and Simulink (MATLAB, 2017a). The parameters used to simulate the drum granulation loop process are listed in Table 1.

Initialization of the mass distribution function inside the granulator is performed using a Gaussian normal distribution function given by Equation 14. For comparison of simulation results, the evolution of the average size of the particles is represented by their d_{50} diameter (median diameter that corresponds to intercept for 50% of cumulative mass).

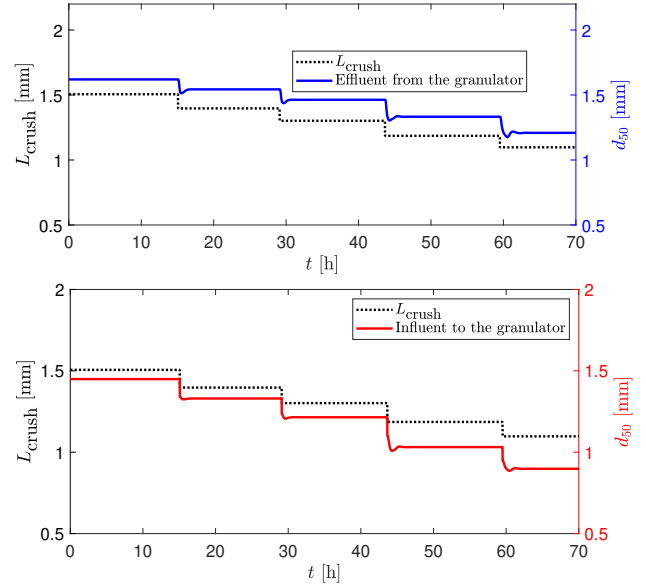


Figure 5: d_{50} of the influent/effluent as a response to the step-by-step change of the crusher gap $L_{\text{crush}} = 1.5 \rightarrow 1.4 \rightarrow 1.3 \rightarrow 1.2 \rightarrow 1.1$ mm.

Table 1: Simulation parameters.

Parameter	Value
Range of L [mm]	0-8
Number of particle classes	80
Length of granulator [m]	10
Number of compartments	3
ρ [$\text{kg} \cdot \text{m}^{-3}$]	1300
β_0 [s^{-1}]	$1.0 \cdot 10^{-13}$
τ [min]	10
$\dot{m}_{\text{sl},i}$ [$\text{kg} \cdot \text{h}^{-1}$]	100
$L_{\text{screen, upp}}$ [mm]	1.5
$L_{\text{screen, low}}$ [mm]	0.9
$K_{\text{eff, upp}}$	45
$K_{\text{eff, low}}$	45
L_{crush} [mm]	1.7-0.3
σ_{crush}	0.25
$X_{\text{sl},i}$	0.05
Time step for RK4 [s]	20

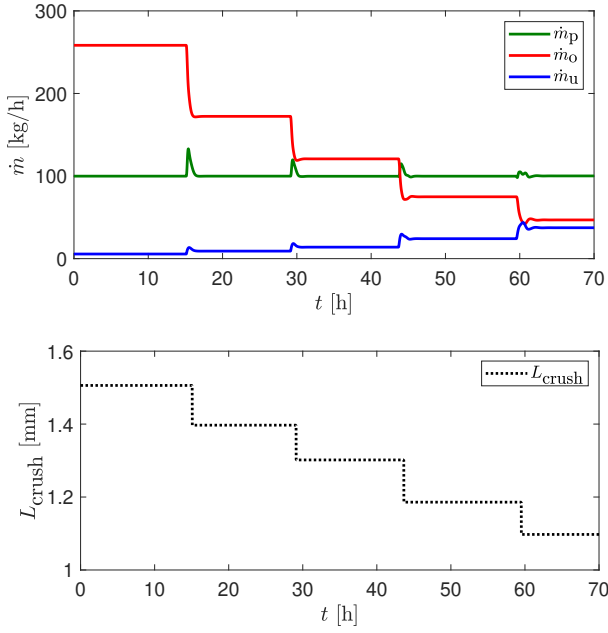


Figure 6: Mass flow rates of over-sized, product-sized and under-sized particles as a response to the step-by-step change of the crusher gap ($L_{\text{crush}} = 1.5 \rightarrow 1.4 \rightarrow 1.3 \rightarrow 1.2 \rightarrow 1.1$ mm).

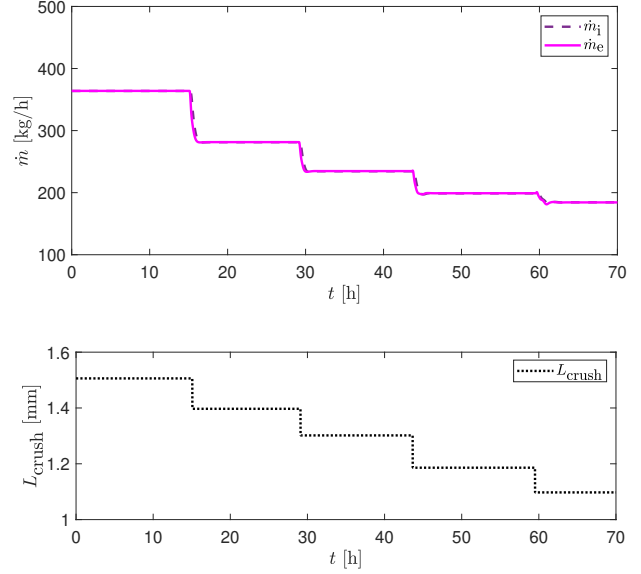


Figure 7: Total mass flow rates of the influent/effluent as a response to the step-by-step change of the crusher gap ($L_{\text{crush}} = 1.5 \rightarrow 1.4 \rightarrow 1.3 \rightarrow 1.2 \rightarrow 1.1$ mm).

4.2 Growth of particles inside the 3-compartment drum granulator

Simulations are performed by applying a 3-compartment drum granulation loop model. This is done to achieve (i) higher accuracy of the developed model, and thus to account for property inhomogeneity inside the granulator, and (ii) the developed granulation loop model will be further used in control studies where spatial discretization is significant to achieve proper system dynamics, e.g., to include some effect of time delay.

Figure 4 shows evolution of particle growth in 3 different compartments of the drum granulator. In the first compartment, particles begin to grow and to collide with each other. In the second compartment, further grow and collision of particles occur. This results in the larger amount of coarser particles in the second compartment of the drum granulator compared to the first one. As particles are transferred to the third compartment, the more time they spend in the granulator, and, thus, the more time they have to agglomerate and to grow. As a result, the third compartment contains the largest amount of coarser particles among all the 3 compartments. The PSD in the flow of the 3rd compartment corresponds to the PSD in the effluent flow from the granulator, that is further sent to screens to

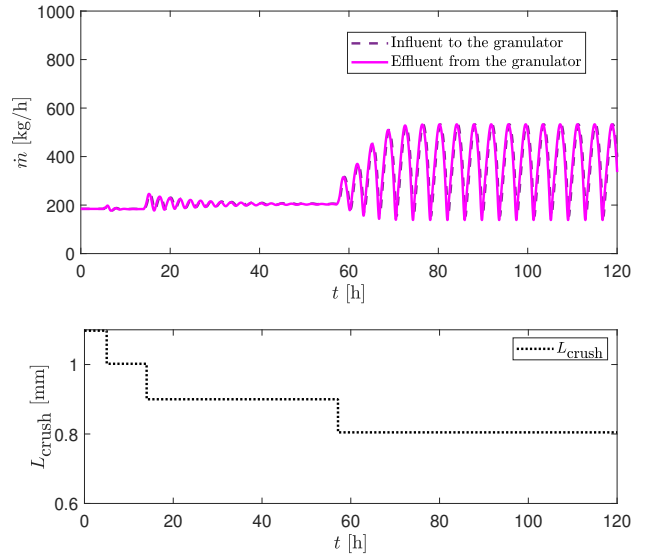


Figure 8: Total mass flow rates of the influent/effluent as a response to the step-by-step change of the crusher gap ($L_{\text{crush}} = 1.1 \rightarrow 1.0 \rightarrow 0.9 \rightarrow 0.8$ mm).

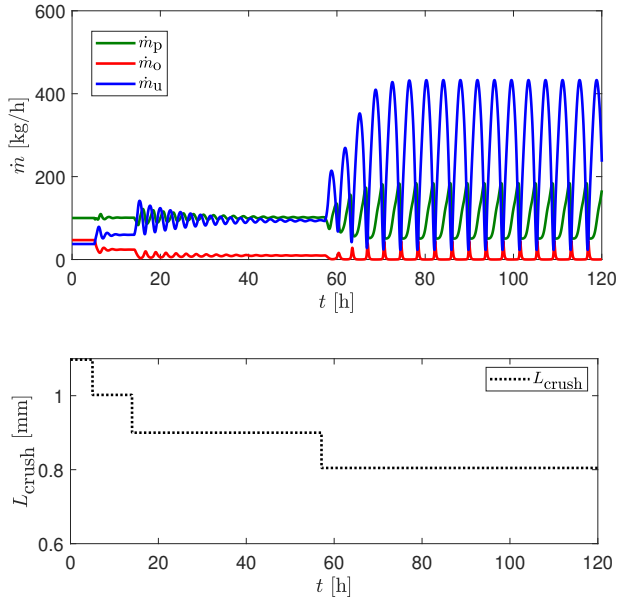


Figure 9: Mass flow rates of over-sized, product-sized and under-sized particles as a response to the step-by-step change of the crusher gap ($L_{\text{crush}} = 1.1 \rightarrow 1.0 \rightarrow 0.9 \rightarrow 0.8$ mm).

separate the flow into the size fractions (under-sized, over-sized, and product-sized particle fractions).

4.3 Effect of crusher gap on granulation loop stability

The dynamic behavior of the granulation loop is inevitably connected with the crusher parameters. In particular, a crusher gap (also called mill grade) plays a significant role in understanding the dynamics of the granulation loop. As is shown in Figure 5, particles are growing inside the drum granulator, and as a result, the average diameter d_{50} of the particles leaving the granulator (effluent) is larger compared to the d_{50} of the particles that are sent to the granulator with the recycle feed (influent).

Stable granulation loop process is observed when a step-by-step change of $L_{\text{crush}} = 1.5 \rightarrow 1.4 \rightarrow 1.3 \rightarrow 1.2 \rightarrow 1.1$ mm are given to the system. This includes stable mass flow rates and d_{50} , for the main granulation loop units, i.e., granulator, screens, crusher (Figure 6 and 7). In particular, stable mass flow rates of both the product-sized particles, off-spec particles, as well as the total mass flow rates in and out of the drum granulator are observed.

Relatively high values of crusher gap spacings ($L_{\text{crush}} > 1.2$ mm) produce larger particles at the outlet of granulator, that therefore results in the higher

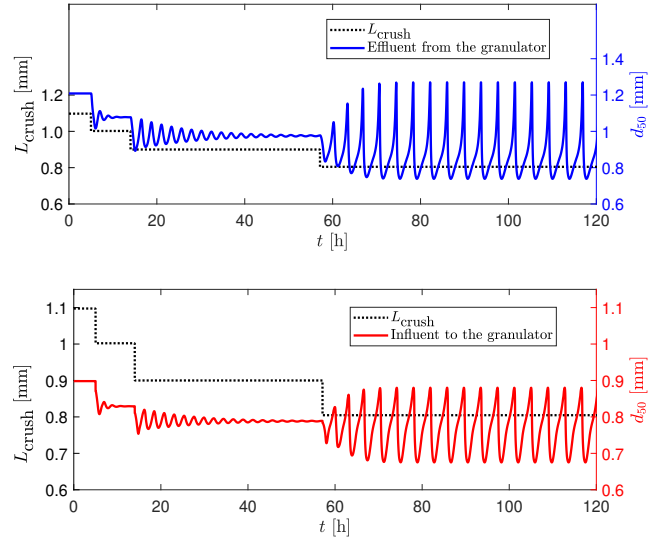


Figure 10: d_{50} of the granulator influent/effluent as a response to a step-by-step change of the crusher gap ($L_{\text{crush}} = 1.1 \rightarrow 1.0 \rightarrow 0.9 \rightarrow 0.8$ mm).

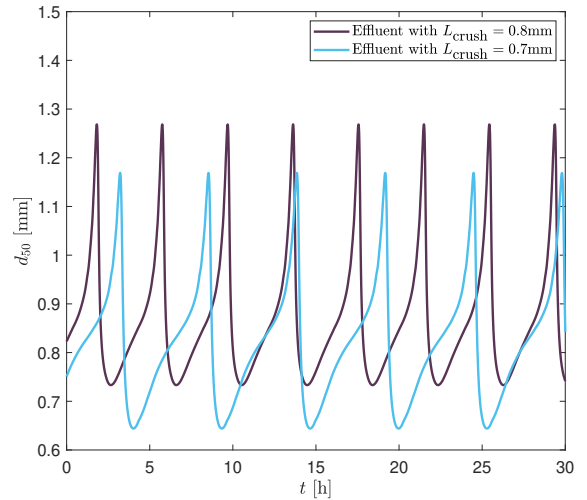


Figure 11: Sustained oscillations at $L_{\text{crush}} = 0.8$ mm versus at $L_{\text{crush}} = 0.7$ mm.

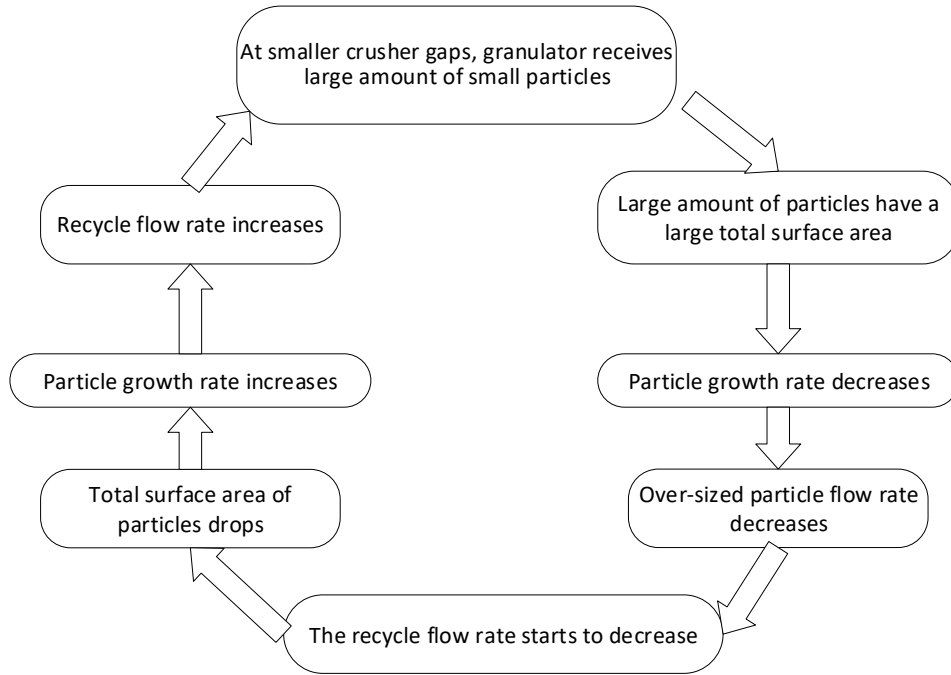


Figure 12: Explanation of the oscillations.

mass flow rate of the over-sized particles leaving the screens. As shown in Figure 6, at crusher gap spacing larger than 1.2 mm, the flow rate of over-sized particles are larger than the product-sized particles. This case is not desirable in industrial granulation plants since less of product is produced. However, over-sized particle flow contributes to the total recycle flow that acts as a seed to the granulator, and hence a larger over-sized fraction maintain the high flow rate of the influent to the drum granulator. Note that separation efficiency K_{eff} of lower and upper screens are set to $\sim 45\%$ that lead to the appearance of the under-sized particles at $L_{\text{crush}} \leq 1.2$ mm. The screen efficiency of $\sim 45\%$ is applied in simulations to achieve higher accuracy of the mathematical model with the real plant operation. In the plant, performance of the screens are *not ideal*, i.e., the under-sized-particles may remain on the upper screen with the over-sized particles and, vice versa, larger particles (e.g., product-sized) may occur in the under-sized fraction. As expected, the smaller the crusher gap is, the smaller is the recycle feed, and the flow of the effluent from the granulator (Figure 7). At smaller crusher gaps, more of the product is produced, and thus, more of particles are collected and taken out from the drum granulation loop.

A decrease in the crusher gap spacing from 1.1 mm to 1.0 mm introduces some damped oscillations in the

process (Figure 8, 9 and 10 at simulation time $t \approx 10$ h). At the latter crusher gap spacing, more of fine particles are produced, as a result of which the mass flow rate of under-sized particles increases (Figure 9), and d_{50} in the recycle feed starts to fluctuate (Figure 10). Consequently, d_{50} of the effluent from the granulator also starts to fluctuate. These fluctuations are not sustained (see simulation time $t \approx 10$ h) and quickly the system reaches stable steady state. As the crusher gap is reduced, more of the under-sized particles are formed, and the amplitude of fluctuations increases. Damped oscillations are observed at 0.9 mm crusher gap when the granulation loop produces similar amount of product as the under-sized particles (see simulation time $t \approx 18$ h). These damped oscillations are seen both in the mass flow rates, as well as in the d_{50} of the granulator influent and effluent. A further step change of L_{crush} to 0.8 mm gives a rise in the amplitude of the oscillations, and consequently, sustained oscillations are observed (see simulation time $t \approx 58$ h).

Interestingly, the period of oscillations changes as crusher gap is changed. In Figure 11, a close look at sustained oscillations for 0.8 mm and 0.7 mm crusher is shown. The period of the sustained oscillations is larger in the case of 0.7 mm crusher gap compared to the case of 0.8 mm crusher gap. Periodic oscillations in

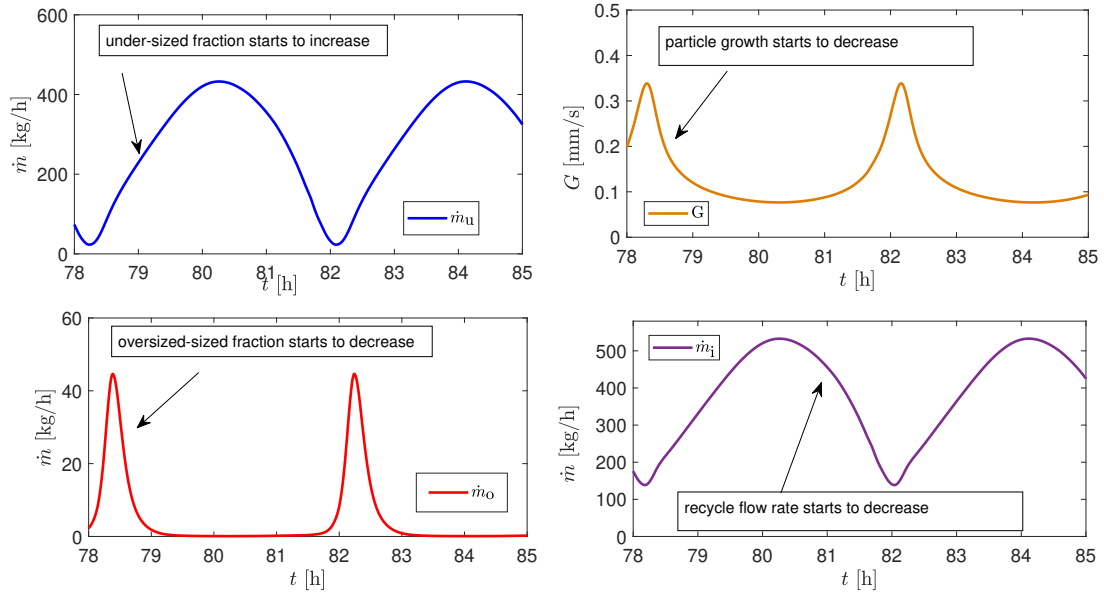


Figure 13: Zoomed oscillations in the process variables.

the granulation loop process can be explained by the recycle stream that is fed back to the granulator. Or, more precisely, with the large amount of fine (under-sized) particles that constitute to a large total surface area of particles in the granulator (Figure 12). For illustration, consider the following numerical example. Assume that there is one particle (sphere) with radius of $r_1 = 1$ mm. This particle will have a volume V_1 and a surface area A_1 as follows:

$$V_1 = \frac{4}{3}\pi r_1^3 = 4.1888e - 09 \quad (22)$$

$$A_1 = 4\pi r_1^2 = 1.2566e - 05. \quad (23)$$

Next, assume that this single particle is crushed into smaller particles of radius $r_2 = \frac{1}{2}r_1$. The volume V_2 and area A_2 of one such smaller particle is

$$V_2 = \frac{4}{3}\pi r_2^3 = 5.2360e - 10 = \frac{1}{8}V_1 \quad (24)$$

$$A_2 = 4\pi r_2^2 = 3.1416e - 06 = \frac{1}{4}A_1. \quad (25)$$

Therefore, for the same volume as the single large particle there will be 8 smaller particles. These 8 smaller particles will have the double surface area compared to the single particle, since $\frac{8}{4}A_1 = 2A_1$

When $L_{\text{crush}} \leq 0.9$ mm, the crusher produces a relatively large amount of crushed fine particles. These fine particles are then combined with the under-sized particles to form the recycle feed. Thus, the recycle feed contains a large amount of fine particles that have

a large surface area. The recycle feed containing large amount of fines is then fed back to the rotary drum. Inside the drum, for the large amount of fine particles with large surface area, the particle growth rate reduces (for a constant supply of the slurry) and the amount of over-sized particle fraction rapidly drops. On the other hand, this rapid drop in the mass flow rate of the over-sized particle fraction leads to a decrease in the total flow rate of the recycle feed (product-sized flow rate, which is not fed back, increases). Due to a lower flow rate of the recycle feed, the drum granulator receives less amount of fine particles per unit time, and consequently, the particle growth rate increases again. This increased particle growth rate results in the beginning of the new cycle of the periodic behavior. In Figure 13, a zoomed region of oscillations is shown. An increase in the under-sized mass flow rate results in a decrease in the growth rate of particles. The decrease in particle rate, in turn, results in the decrease of the over-sized mass flow rate. As a consequence the recycle feed decreases.

4.4 Effect of slurry feed on granulation loop stability

As discussed in Section 4.3, the high total surface area of large amount of fine particles limits the growth rate of particles. Consequently, particles do not grow sufficiently fast to form large particles. Thus, by increasing the slurry feed, the process might become more stable. To illustrate this, simulations are also performed with

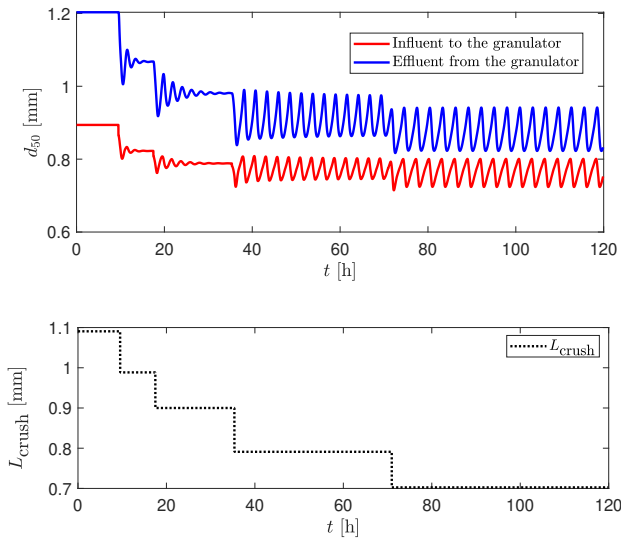


Figure 14: d_{50} as a response to the step-by step change of L_{crush} with $\dot{m}_{\text{slurry}} = 500$ kg/h.

the increased slurry flow rate.

Simulation results show that an increase in the mass flow rate of slurry improve the stability of the process (Figure 14 and 15). Periodic oscillations with the increased slurry flow rate appear at smaller crusher gap compared to the simulation results with the original value of the slurry flow rate. When the slurry feed \dot{m}_{sl} is increased to 500 kg/h (Figure 14), significantly less oscillations (more damped oscillations) are observed at $L_{\text{crush}} \leq 0.8$ mm compared to the original case with $\dot{m}_{\text{sl}} = 100$ kg/h (Figure 10).

Simulations with $\dot{m}_{\text{sl}} = 1000$ kg/h (Figure 15) show even more stable process having only a few fluctuations even at very small crusher gaps of 0.5 mm. Typically, for granulation plants, it is important to maintain a constant solid-to-liquid ratio. The constant solid-to-liquid ratio assures product quality requirements, e.g., moisture content, dustiness, flow-ability, etc., and thus, slurry feed is usually kept constant and is not changed during the operation. In addition, increased slurry feed may result in over-wetting of the particles, i.e., particles will not stick together and will not grow. Consequently, for stable granulation loop operation, at least the crusher gap spacing should be monitored systematically.

5 Conclusions

A dynamic model for rotary drum granulation loop is presented in this paper. For the analysis of dynamic behavior, a mass based population balance equation

using particle diameter as the internal coordinate and granulator length as the external coordinate is developed. The drum granulation loop model is able to capture two granulation mechanisms: particle growth due to layering and particle size change due to binary agglomeration. Simulation results of a granulation loop having a 3-compartment rotary drum model show that the crusher gap spacing has a significant influence on the overall stability of the granulation loop. At larger crusher gap spacings, a stable granulation process is observed. However, as the crusher gap spacing is reduced, the granulation loop starts to show oscillatory behavior, and at a certain reduced crusher gap spacing, sustained periodic oscillations occur. The reason of the occurring oscillations is the off-spec particle flow that is recycled to the granulator and acts as nuclei for the new granule generation. At smaller crusher gap spacings, the granulator receives large amount of fines with the recycle feed. In the granulator, large amount of fines have a large total particle surface that slows down the particle growth. Thus, the growth rate and d_{50} of particles decreases. On the other hand, slower growth rate contributes to the rapid drop in the production of coarse (over-sized) particles, that in turn, reduce the total recycle feed to the granulator. As a result, the granulator receives smaller amount of fine particles that now have smaller particle total surface area. Thus, the growth rate and d_{50} of particles again increases and gives the start of the new cycle of periodic oscillations. To illustrate the effect of deficiency of slurry feed on the total granulation loop stability, simulations are also performed with the increased slurry feed. These simulation results show that increased slurry feed has a positive effect on overall stability of the loop. The higher the flow rate of slurry is, the less oscillations occur. However, the increased slurry feed may result in over-wetting of the particles, and as a result the particles will not stick to each other (agglomerate). Therefore, crusher gap and slurry feed influence the stability of the granulation loop, and both should be properly controlled during granulation loop operation. The developed dynamic granulation loop model in this study can be further used to develop control strategies for granulation loops applicable to different configurations of such loops.

Acknowledgments

The economic support from The Research Council of Norway and Yara Technology Centre through project no. 269507/O20 'Exploiting multi-scale simulation and control in developing next generation high efficiency fertilizer technologies (HEFTY)' is gratefully acknowledged.

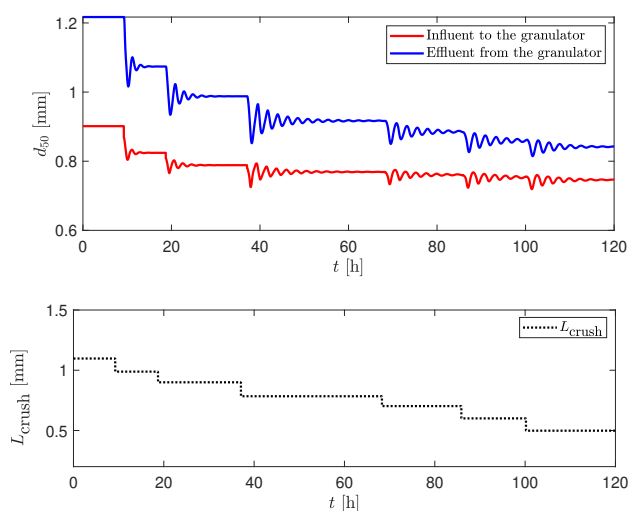


Figure 15: d_{50} as a response to the step-by step change of L_{crush} with $\dot{m}_{slurry} = 1000$ kg/h.

References

- Bück, A., Dürr, R., Schmidt, M., and Tsotsas, E. Model predictive control of continuous layering granulation in fluidised beds with internal product classification. *Journal of Process Control*, 2016. 45:65–75. doi:[10.1016/j.jprocont.2016.07.003](https://doi.org/10.1016/j.jprocont.2016.07.003).
- Cameron, I., Wang, F., Immanuel, C., and Stepanek, F. Process systems modelling and applications in granulation: A review. *Chemical Engineering Science*, 2005. 60(14):3723–3750. doi:[10.1016/j.ces.2005.02.004](https://doi.org/10.1016/j.ces.2005.02.004).
- Drechsler, J., Peglow, M., Heinrich, S., Ihlow, M., and Mörl, L. Investigating the dynamic behaviour of fluidized bed spray granulation processes applying numerical simulation tools. *Chemical Engineering Science*, 2005. 60(14):3817–3833. doi:[10.1016/j.ces.2005.02.010](https://doi.org/10.1016/j.ces.2005.02.010).
- Heinrich, S., Peglow, M., Ihlow, M., and Mörl, L. Particle population modeling in fluidized bed-spray granulation analysis of the steady state and unsteady behavior. *Powder Technology*, 2003. 130(1-3):154–161. doi:[10.1016/S0032-5910\(02\)00259-0](https://doi.org/10.1016/S0032-5910(02)00259-0).
- Herce, C., Gil, A., Gil, M., and Cortés, C. A cape-taguchi combined method to optimize a npk fertilizer plant including population balance modeling of granulation-drying rotary drum reactor. In *Computer Aided Chemical Engineering*, volume 40, pages 49–54. Elsevier, 2017. doi:[10.1016/B978-0-444-63965-3.50010-6](https://doi.org/10.1016/B978-0-444-63965-3.50010-6).
- Hounslow, M., Ryall, R., and Marshall, V. A discretized population balance for nucleation, growth, and aggregation. *AIChE Journal*, 1988. 34(11):1821–1832. doi:[10.1002/aic.690341108](https://doi.org/10.1002/aic.690341108).
- Hulburt, H. and Katz, S. Some problems in particle technology: A statistical mechanical formulation. *Chemical Engineering Science*, 1964. 19(8):555–574.
- Iveson, S., Litster, J., Hapgood, K., and Ennis, B. Nucleation, growth and breakage phenomena in agitated wet granulation processes: a review. *Powder technology*, 2001. 117(1-2):3–39. doi:[10.1016/S0032-5910\(01\)00313-8](https://doi.org/10.1016/S0032-5910(01)00313-8).
- Kapur, P. Kinetics of granulation by non-random coalescence mechanism. *Chemical Engineering Science*, 1972. 27(10):1863–1869. doi:[10.1016/0009-2509\(72\)85048-6](https://doi.org/10.1016/0009-2509(72)85048-6).
- Koren, B. A robust upwind discretization method for advection, diffusion and source terms. In C. B. Vreugdenhil and B. Koren, editors, *Numerical Methods for Advection-Diffusion Problems, Notes on Numerical Fluid Mechanics*, pages 117–138. 1993.
- Kumar, J. *Numerical approximations of population balance equations in particulate systems*. Ph.D. thesis, Otto-von-Guericke-Universität Magdeburg, Universitätsbibliothek, 2006.
- Kumar, J., Peglow, M., Warnecke, G., Heinrich, S., and Mörl, L. Improved accuracy and convergence of discretized population balance for aggregation: The cell average technique. *Chemical Engineering Science*, 2006. 61(10):3327–3342. doi:[10.1016/j.ces.2005.12.014](https://doi.org/10.1016/j.ces.2005.12.014).
- Kumar, S. and Ramkrishna, D. On the solution of population balance equations by discretization -I. A fixed pivot technique. *Chemical Engineering Science*, 1996. 51(8):1311–1332. doi:[10.1016/0009-2509\(96\)88489-2](https://doi.org/10.1016/0009-2509(96)88489-2).
- Litster, J. and Ennis, B. *The science and engineering of granulation processes*, volume 15. Springer Science & Business Media, 2004.
- MATLAB. The MathWorks, Inc., Natick, Massachusetts, United States., 2017a.
- Molerus, O. and Hoffmann, H. Darstellung von wind-sichtertrennkurven durch ein stochastisches modell. *Chemie Ingenieur Technik*, 1969. 41(5-6):340–344. doi:[10.1002/cite.330410523](https://doi.org/10.1002/cite.330410523).
- Mörl, L. *Anwendungsmöglichkeiten und Berechnung von Wirbelschichtgranulationstrocknungsanlagen*. Ph.D. thesis, Technische Hochschule Magdeburg, 1981.

- Mörl, L., Mittelstrab, M., and Sachse, J. Zum Kugelwachstum bei der Wirbelschichttrocknung von Suspensionen oder Lösungen. *Chemical Technology*, 1977. 29(10):540–541.
- Radichkov, R., Müller, T., Kienle, A., Heinrich, S., Peglow, M., and Mörl, L. A numerical bifurcation analysis of continuous fluidized bed spray granulator with external product classification. *Chemical Engineering and Processing*, 2006. 45:826–837. doi:[10.1016/j.cep.2006.02.003](https://doi.org/10.1016/j.cep.2006.02.003).
- Ramachandran, R. and Chaudhury, A. Model-based design and control of a continuous drum granulation process. *Chemical Engineering Research and Design*, 2012. 90(8):1063–1073. doi:[10.1016/j.cherd.2011.10.022](https://doi.org/10.1016/j.cherd.2011.10.022).
- Ramachandran, R., Immanuel, C. D., Stepanek, F., Litster, J. D., and Doyle III, F. J. A mechanistic model for breakage in population balances of granulation: Theoretical kernel development and experimental validation. *Chemical Engineering Research and Design*, 2009. 87(4):598–614. doi:[10.1016/j.cherd.2008.11.007](https://doi.org/10.1016/j.cherd.2008.11.007).
- Ramkrishna, D. *Population balances: Theory and applications to particulate systems in engineering*. Academic press, 2000.
- Valiulis, G. and Simutis, R. Particle growth modelling and simulation in drum granulator-dryer. *Information Technology and Control*, 2009. 38(2).
- Vesjolaja, L., Glemmestad, B., and Lie, B. Population balance modelling for fertilizer granulation process. *Proceedings of The 59th Conference on Simulation and Modelling (SIMS 59), 26-28 September 2018, Oslo Metropolitan University, Norway*, 2018. doi:[10.3384/ecp1815395](https://doi.org/10.3384/ecp1815395).
- Wang, F., Ge, X., Balliu, N., and Cameron, I. Optimal control and operation of drum granulation processes. *Chemical Engineering Science*, 2006. 61(1):257–267. doi:[10.1016/j.ces.2004.11.067](https://doi.org/10.1016/j.ces.2004.11.067).